

Bulk two-dimensional Pauli-limited superconductorT. Coffey,¹ C. Martin,¹ C. C. Agosta,¹ T. Kinoshita,² and M. Tokumoto^{2,3}¹*Department of Physics, Clark University, Worcester, Massachusetts 01610, USA*²*CREST, JST, Kawaguchi 332-0012, Japan*³*Nanotechnology Research Institute, AIST, Tsukuba 305-8568, Japan*

(Received 2 September 2010; published 2 December 2010)

We present a nearly perfect Pauli-limited critical-field phase diagram for the anisotropic organic superconductor α -(ET)₂NH₄(SCN)₄ when the applied magnetic field is oriented parallel to the conducting layers. The critical fields (H_{c2}) were found by use of penetration depth measurements. Because H_{c2} is Pauli limited, the size of the superconducting energy gap can be calculated. The role of spin-orbit scattering and many-body effects play a role in explaining our measurements.

DOI: 10.1103/PhysRevB.82.212502

PACS number(s): 74.70.Kn, 74.25.Dw

Over the past 40 years there have been many theoretical calculations¹⁻⁵ and experiments on layered superconductors⁶⁻¹² subjected to an external magnetic field applied parallel to the conducting layers. When the magnetic field is precisely aligned parallel to the conducting layers, magnetic flux lines effectively penetrate the least conducting layers between the conducting planes and the orbital destruction of superconductivity associated with the vortices is suppressed.

In this case, the superconductor can be described as a series of Josephson-coupled layers (JCLs) as long as the temperature is below the two-dimensional (2D)/three-dimensional (3D) transition temperature ($T < T^*$) that occurs when the coherence length perpendicular to the layers (ξ_o^\perp) is less than the distance between the layers. In the parallel orientation, the Cooper pairs will be broken for a typical superconductor when the energy gained by being in the superconducting state equals the energy cost of maintaining antiparallel spins in an applied field. This limit is known as the Clogston-Chandrasekar or Pauli paramagnetic limit. The upper critical field (H_{c2}) for a Pauli-limited superconductor is $H_P = \frac{\sqrt{2}\Delta_o}{g\mu_B}$, where Δ_o is the energy gap, g is the Landé g factor, and μ_B is the Bohr magneton.¹³ For a BCS superconductor $\mu_o H_P^{\text{BCS}} = 1.84 \text{ T/K } T_c$. Many investigations of layered superconductors have focused on the possibility of realizing an exotic, inhomogeneous state known as the Fulde-Ferrell-Larkin-Ovchinnikov state,^{14,15} which allows H_{c2} to exceed H_P .

In this Brief Report we present a Pauli-limited critical-field phase diagram with the applied field parallel to the conducting layers ($\mu_o H \parallel ac$ plane) for the anisotropic organic superconductor α -(ET)₂NH₄(SCN)₄ (short form ET-NH4).¹⁶ Our phase diagram is based on rf penetration depth measurements that utilize a tunnel diode oscillator (TDO).^{17,18} The phase diagram we present is a close match to the calculations from Klemm *et al.*² in the limit of small spin-orbit scattering, and the low-temperature H_{c2} we measure is a close match to the many-body prediction from McKenzie.¹⁹ The remarkable result is that due to Pauli-limiting, H_{c2} tracks the superconducting energy gap at all temperatures. In contrast to other organic superconductors,²⁰⁻²³ we observe no evidence of H_{c2} exceeding the Pauli limit in ET-NH4.

Previous attempts to synthesize and measure a bulk Pauli-limited superconductor have been stymied by materials that have low anisotropy or weak spin-orbit scattering.⁷ Other

investigations may have been limited by the available magnetic fields and low temperatures at the time of the experiments.¹² A convincing Pauli-limited superconductor was realized for a single layer of aluminum.²⁴

Despite having a low T_c [$\approx 0.9 \text{ K}$ (Refs. 25–28)], ET-NH4 is an ideal material to study because it is one of the most anisotropic layered superconductors and should be a model JCL superconductor. The anisotropy parameter (γ) for ET-NH4=2000, while $\gamma=150$ for Bi₂Sr₂CaCu₂O_{8+ δ} .²⁷ The high anisotropy in ET-NH4 produces a broad, zero-field resistive transition [reported onset temperatures vary from 1.2 to 2.4 K (Refs. 27–32)], a broad peak in the zero-field specific heat at T_c ,²⁵⁻²⁷ anisotropic penetration depths ($\lambda_\perp = 1400 \mu\text{m}$ and $\lambda_\parallel = 0.7 \mu\text{m}$ as $T \rightarrow 0$,²⁷ and anisotropic resistivity [$20 \leq \rho_\perp \leq 40 \Omega \text{ cm}$ and $10 \leq \rho_\parallel \leq 100 \mu\Omega \text{ cm}$ at 3 K (Ref. 27)].

In a TDO experiment we measure the amplitude (A) and frequency shift (ΔF) of a self-resonant circuit with unperturbed frequency F_o . These quantities are determined by the complex impedance of the coil containing the sample (L'). For the case of a long rod in an axial coil, $L' = L_o(1 + 4\pi\eta\{\chi' - j\chi''\})$, where η is defined as the volume filling factor, directly related to the penetration depth. As the rf field is expelled from the sample, η changes and thus A and ΔF , related to χ' and χ'' shift together. The region where η dominates is called the skin depth region.³³ The sample we characterized is a small block (1.69 mm \times 1.83 mm \times 1.0 mm), not a long rod; therefore, L' must be corrected by a demagnetization factor in order to measure absolute quantities. We did not measure the demagnetization factor of our sample and do not report absolute values for the penetration depth. However, the temperature or applied field at which a transition occurs is clear in our measurements.

In type II superconductors, a complex penetration depth ($\tilde{\lambda}$) includes the normal skin depth (δ), the London penetration depth (λ_L), and the Campbell penetration depth (λ_c).^{9,34,35} As the applied field is increased the following occurs: the flux lattice is destroyed, λ_L diverges at H_{c2} , and $\tilde{\lambda}$ becomes limited by δ . From our data, we define H_{c2} via the maximum in the second derivative of the frequency response of the TDO (ΔF) with respect to the applied field and is calculated for fields above and below H_{c2} .

The phase diagram we present is constructed from three different experimental runs, two at the NHMFL and one at

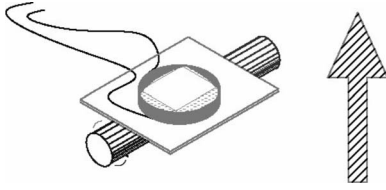


FIG. 1. Schematic of coil and sample on a rotating platform. The large arrow indicates the direction of the applied field. The cylinder is the axis of rotation.

Clark University, using three different circuits, where $F_0 \approx 25$ MHz, 10 MHz, 35 MHz respectively. All three experimental runs produced consistent results. The parallel orientation is determined from the sharp cusp in H_{c2} versus angle. At Clark University, a transverse 1 T electromagnet, single-shot He³ refrigerator, and rotating probe with an angular resolution of 0.1° were used. At the NHMFL a 18 T superconducting magnet, dilution refrigerator, and rotating probe with an angular resolution of 0.050° were used.³⁶ In all cases the sample is placed in a small coil that is part of a self-resonant circuit. Small balls of cotton are packed between the sample and the coil and a Teflon gurney is tied around the coil and the rotating platform to hold the sample in place. The flattest side of the sample sits on a rotating platform such that the conducting (ac) planes are roughly parallel to the platform and perpendicular to the axis of the coil, as in Fig. 1. The platform's axis of rotation is roughly parallel to either the a or c crystallographic direction of the sample. The rf coil excites currents in the conducting planes of the sample. Using $\rho_{||}$ from Ref. 27, $\delta_{||} = 70$ μm at 25 MHz and 3 K. The rf field generated by the coil is ≤ 70 μT .

In addition to the parallel and perpendicular phase diagrams, we found $T_c \approx 0.96$ K from temperature sweeps at Clark University. In the normal state the TDO measures resistivity, which as a function of magnetic field exhibits Shubinkov-de Haas (SdH) oscillations.³⁷ From these SdH oscillations we extracted Fermi-surface parameters such as: the SdH frequency, $F_{\text{SdH}} = 564 \pm 2$ T, the effective mass, $m^* = 2.5m_e$, and the Dingle temperature $T_D = 1.11$ K, which can be directly translated into a scattering rate via $\frac{1}{\tau} = 2\pi k_b T_D / \hbar$. From our SdH data, we find $\ell = 681$ \AA and $\tau = 1.09$ ps, where ℓ is the mean-free path of the conducting quasiparticles. These results are consistent with previous results.³⁸ From the perpendicular, zero-temperature critical field [$\mu_0 H_{c2}^\perp(0) = 0.13$ T] we calculated the coherence length for quasiparticles in the conducting layers, $\xi_o^\parallel = 500$ \AA . To the best of our knowledge, a previously reported value ($\xi_o^\parallel = 500$ \AA) was calculated from the slope [$\frac{d(\mu_0 H_{c2})}{dT} \Big|_{T_c} = -0.08 \pm 0.02$ T/K] of a perpendicular phase diagram generated via specific heat data.²⁷ For a superconductor, the dirty limit is defined when $\ell \ll \xi_o^\parallel$. Given that $\ell / \xi_o^\parallel \approx 1.4$, ET-NH4 resides just on the clean side of the boundary between a clean and dirty superconductor.

Figure 2 shows amplitude and frequency data for field sweeps in the parallel and perpendicular orientations. This experiment is in the skin depth regime because $\delta / r_s \approx 0.04$. Figure 2(a) suggests that we observe Campbell penetration in the perpendicular orientation because $\frac{\Delta F}{F_0} \propto \sqrt{H}$ at low fields.

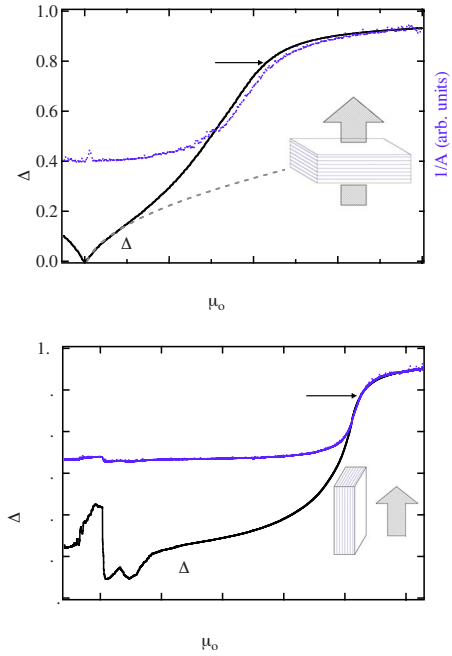


FIG. 2. (Color online) Comparison of $\frac{|\Delta F|}{F_0}$ and $\frac{1}{A}$ versus applied field. As a result of being in the skin depth limit, just below and above H_{c2} , $\frac{1}{A}$, and $\frac{|\Delta F|}{F_0}$ change in an almost identical manner. The dashed line in Fig. 2(a) is a square-root fit to the low field frequency data. In order to emphasize the correlation between the frequency and amplitude data $|\Delta F|$ is plotted instead of ΔF . As the field increases the frequency actually decreases. The inset shows the orientation of the applied field with respect to the conducting layers.

There is very little structure in the amplitude signal at low field because the coil resistance dominates Q_{tc} .

Microscopic calculations in the clean³⁹ and dirty² limits have predicted specific phase diagrams for JCL superconductors. For a clean, JCL superconductor with negligible spin-orbit scattering ($\tau_{\text{so}} \rightarrow \infty$), Ref. 39 predicts that $H_{c2}^\parallel = H_P^{\text{BCS}} \sqrt{1 - T/T_c}$ when the temperature is below the 2D/3D transition ($T < T^*$). For a dirty, JCL superconductor with strong spin-orbit scattering ($\tau_{\text{so}} \rightarrow 0$), H_{c2} may reach up to six times H_P (Ref. 2) according to

$$H_{c2}^\parallel(0) = 0.602(k_b T_c \tau_{\text{so}} / \hbar)^{-1/2} H_P^{\text{BCS}}. \quad (1)$$

In a dirty system with no spin-orbit scattering ($\tau_{\text{so}} \rightarrow \infty$), H_{c2} saturates near H_P .²

A relevant complication is that two mechanisms can enhance H_P^{BCS} —strong coupling and many-body effects. Many-body effects can increase H_P for a spin-singlet Fermi liquid with a quasi-2D circular Fermi surface by the factor R , $H_P = \frac{H_P^{\text{BCS}}}{R}$, where R is Wilson's ratio.¹⁹ A theory-independent method to estimate the many-body enhancement has also been proposed.^{8,40} This method equates the condensation energy of the superconductor and the energy gained by having the electrons' spin align with the applied field.

The low concentration of conducting quasiparticles in the organic superconductors promotes strong interactions among the carriers and H_P may well be enhanced by many-body effects. Wilson's ratio (R) for ET-NH4 is 0.7 ± 0.2 or

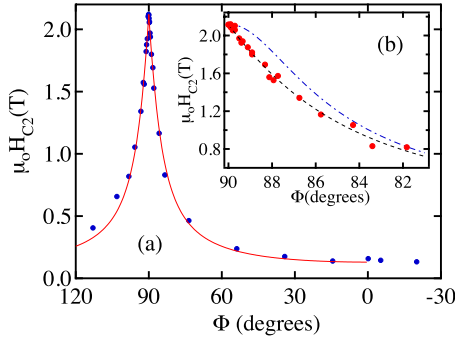


FIG. 3. (Color online) H_{c_2} as a function of angle at 40 mK. The solid line is a fit to Eq. (2) using the measured $H_{c_{2\perp}}$ and $H_{c_{2\parallel}}$ as fitting parameters. Inset: the dashed line is the same fit to Eq. (2) as the main figure, and the dotted-dashed line is a fit to the anisotropic G-L theory. The angle (Φ) between the normal of the conducting layer and the applied field is zero when the applied field is perpendicular to the conducting layers.

0.86 ± 0.05 .¹⁹ Using the value of R with the smaller uncertainty and $H_P^{\text{BCS}} = 1.77$, $\frac{H_P}{H_P^{\text{BCS}}} = 1.17 \pm 0.07$. Using the jump in specific-heat data^{25–27} to estimate the condensation energy and susceptibility,⁴¹ we estimate H_P using the theory-independent method.⁸ This method depends on which set of specific-heat data is used, and produces a high and low estimate very similar to the many-body theory using Wilson's ratio. In both cases the low estimates predict $\frac{H_P}{H_P^{\text{BCS}}} = 1.2$, which matches the ratio of the measured zero-temperature H_{c_2} and H_P^{BCS} .

The inherent assumptions in the JCL theories presented in Refs. 2 and 39 assume a weakly coupled, s -wave superconductor. In contrast to many other organic superconductors, specific-heat data show that ET-NH4 is a weakly coupled superconductor.⁴² Even though d -wave symmetry has been proposed in the κ phase organic superconductors and p -wave symmetry clearly shown in some Bechgaard salts,¹⁰ there has been no data indicating anything besides a conventional order parameter in ET-NH4.

The inherent 2D nature of our sample suggests that it is below T^* over most of the temperature range. It is expected that the angular dependence of H_{c_2} follows the bell-like anisotropic G-L equation, $H_{c_2}^2 \left[\left(\frac{\cos(\Phi)}{H_{c_{2\perp}}} \right)^2 + \left(\frac{\sin(\Phi)}{H_{c_{2\parallel}}} \right)^2 \right] = 1$, above T^* and the cusp-like Tinkham thin-film equation,

$$\left| \frac{H_{c_2}(\Phi)\cos(\Phi)}{H_{c_{2\perp}}} \right| + \left[\frac{H_{c_2}(\Phi)\sin(\Phi)}{H_{c_{2\parallel}}} \right]^2 = 1, \quad (2)$$

below T^* .⁴

For a truly Pauli-limited superconductor even Eq. (2) should not be valid because it is still based on orbital destruction of superconductivity. However, one can argue phenomenologically that a similar equation should exist with H_P in place of H_{c_2} parallel. A theoretical argument for this phenomenological equation was made by Bulaevskii.⁴³ When the sample is within a fraction of a degree of parallel, the H_{c_2} should deviate from any of these equations, and this phenomena was seen in recent studies.²¹ To ensure that the par-

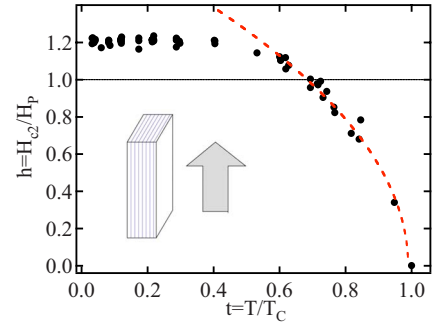


FIG. 4. (Color online) The phase diagram, with the applied field parallel to the conducting layers, plotted in reduced coordinates ($h = \frac{H_{c_2}}{H_P^{\text{BCS}}}$, $t = \frac{T}{T_C}$). The dashed line is a fit to the data where $h \propto \sqrt{1-t}$. The solid line indicates H_P^{BCS} . The inset shows the orientation of the applied field with respect to the conducting layers.

allel critical fields we report are accurate, seven full angular studies were conducted between 40 and 750 mK. Below 750 mK our data fit very well to the Tinkham thin film equation [Eq. (2)]. Figure 3(a) plots H_{c_2} as a function of angle at 40 mK. A comparison between the data and the predictions for a layered superconductor in the 2D and 3D limiting cases is made in Fig. 3(b) at angles close to the parallel orientation. The agreement between our data and the Tinkham thin-film equation indicates that the vortices in each layer are decoupled and ET-NH4 is a JCL superconductor.

Finally, in Fig. 4 we present the phase diagram we measured in reduced coordinates, where $t = \frac{T}{T_C}$ and $h = \frac{H_{c_2}}{H_P^{\text{BCS}}}$. This phase diagram has the essential features of a superconductor in the Pauli limit. The critical field follows the temperature dependence of the energy gap, starting out with a square root dependence near T_c [$H_{c_2} \propto (1-t)^{1/2}$] and approaching a constant by $t=0.4$. The low-temperature section of this phase diagram is striking because the low-temperature critical fields are saturated at 2.15 T, which is 20% above H_P^{BCS} , in agreement with our Wilson's ratio calculation. There is some data in a study using thermal conductivity that supports our phase diagram,⁴⁴ and we have recently repeated our experiment with a sample from a different sample grower,⁴⁵ and a new TDO, with results that are within the scatter of the present data.

One can estimate τ_{so} using a qualitative comparison between the phase diagram in Fig. 4 and Fig. 9 of Ref. 2 and $\tau_{\text{so}} = \infty$ or if one uses Eq. (1) and assumes that all of the enhancement of H_{c_2} in ET-NH4 is due to spin-orbit scattering $\tau_{\text{so}} = 2.0$ ps. In this case it is difficult to know whether the enhancement in H_{c_2} is due to many-body effects, spin-orbit scattering or a combination of the two. Because τ_{so} is at least twice as great as τ , it is more likely that the effects of spin-orbit scattering are small to negligible. In the case that spin-orbit scattering is negligible, $\Delta_o = 2.0 \times 10^{-23}$ J per Cooper pair.

We acknowledge H. Gao, J. Norton, T. Murphy, E. Palm, and S. Hannahs for help doing these experiments, R. Klemm and J. Singleton for useful discussions, L. Rubin for donated equipment from the FBNML, and NSF under Grant No. 9805784 and DOE under Grant No. ER46214 for support.

- ¹W. E. Lawrence and S. Doniach, in *Proceedings of the Twelfth International Conference on Low-Temperature Physics, Kyoto, 1970*, edited by E. Kanada (Academic Press of Japan, Kyoto, 1971), p. 361.
- ²R. A. Klemm, A. Luther, and M. R. Beasley, *Phys. Rev. B* **12**, 877 (1975).
- ³L. N. Bulaevskii, *Zh. Eksp. Teor. Fiz.* **65**, 1278 (1973) [*Sov. Phys. JETP* **38**, 634 (1974)].
- ⁴T. Schneider and A. Schmidt, *Phys. Rev. B* **47**, 5915 (1993).
- ⁵A. G. Lebed and K. Yamaji, *Phys. Rev. Lett.* **80**, 2697 (1998).
- ⁶P. W. Adams, *Phys. Rev. Lett.* **92**, 067003 (2004).
- ⁷C. Strunk, C. Stürgers, U. Paschen, and H. v. Löhneysen, *Phys. Rev. B* **49**, 4053 (1994).
- ⁸F. Zuo, J. S. Brooks, R. H. McKenzie, J. A. Schlueter, and J. M. Williams, *Phys. Rev. B* **61**, 750 (2000).
- ⁹P. A. Mansky, P. M. Chaikin, and R. C. Haddon, *Phys. Rev. Lett.* **70**, 1323 (1993).
- ¹⁰I. J. Lee, M. J. Naughton, G. M. Danner, and P. M. Chaikin, *Phys. Rev. Lett.* **78**, 3555 (1997).
- ¹¹W. K. Kwok, U. Welp, K. D. Carlson, G. W. Crabtree, K. G. Vandervoort, H. H. Wang, A. M. Kini, J. M. Williams, D. L. Stupka, L. K. Montgomery, and J. E. Thompson, *Phys. Rev. B* **42**, 8686 (1990).
- ¹²D. E. Prober, R. E. Schwall, and M. R. Beasley, *Phys. Rev. B* **21**, 2717 (1980).
- ¹³A. M. Clogston, *Phys. Rev. Lett.* **9**, 266 (1962).
- ¹⁴P. Fulde and R. A. Ferrell, *Phys. Rev.* **135**, A550 (1964).
- ¹⁵A. I. Larkin and Y. N. Ovchinnikov, *Zh. Eksp. Teor. Fiz.* **47**, 1136 (1964) [*Sov. Phys. JETP* **20**, 762 (1965)].
- ¹⁶The initial motivation for this experiment was two phase diagrams that contradicted each other (Refs. 29 and 31).
- ¹⁷T. Coffey, Z. Bayindir, J. F. DeCarolis, M. Bennett, G. Esper, and C. C. Agosta, *Rev. Sci. Instrum.* **71**, 4600 (2000).
- ¹⁸C. H. Mielke and J. Singleton, *J. Phys.: Condens. Matter* **13**, 8325 (2001).
- ¹⁹R. H. McKenzie, [arXiv:cond-mat/9905044](https://arxiv.org/abs/cond-mat/9905044) (unpublished).
- ²⁰C. C. Agosta, C. Martin, H. A. Radovan, E. C. Palm, T. P. Murphy, S. W. Tozer, J. C. Cooley, J. A. Schlueter, and C. Petrovic, *J. Phys. Chem. Solids* **67**, 586 (2006).
- ²¹W. A. Coniglio, L. E. Winter, K. Cho, C. C. Agosta, B. Fravel, and L. K. Montgomery, [arXiv:1003.6088](https://arxiv.org/abs/1003.6088) (unpublished).
- ²²K. Cho, B. E. Smith, W. A. Coniglio, L. E. Winter, C. C. Agosta, and J. A. Schlueter, *Phys. Rev. B* **79**, 220507(R) (2009).
- ²³R. Lortz, Y. Wang, A. Demuer, P. H. M. Böttger, B. Bergk, G. Zwiczak, Y. Nakazawa, and J. Wosnitza, *Phys. Rev. Lett.* **99**, 187002 (2007).
- ²⁴P. M. Tedrow and R. Meservey, *Phys. Rev. B* **8**, 5098 (1973).
- ²⁵B. Andraka, G. R. Stewart, K. D. Carlson, H. H. Wang, M. D. Vashon, and J. M. Williams, *Phys. Rev. B* **42**, 9963 (1990).
- ²⁶Y. Nakazawa, A. Kawamoto, and K. Kanoda, *Phys. Rev. B* **52**, 12890 (1995).
- ²⁷H. Taniguchi, Y. Nakazawa, and K. Kanoda, *Phys. Rev. B* **57**, 3623 (1998).
- ²⁸H. H. Wang, K. D. Carlson, U. Geiser, W. K. Kwok, M. D. Vashon, J. E. Thompson, N. F. Larsen, G. D. McCabe, R. S. Hulscher, and J. M. Williams, *Physica C* **166**, 57 (1990).
- ²⁹J. S. Brooks, S. Uji, H. Aoki, T. Terashima, M. Tokumoto, N. Kinoshita, Y. Tanaka, and H. Anzai, *Synth. Met.* **70**, 839 (1995).
- ³⁰Y. Shimojo, T. Ishiguro, T. Toita, and J. Yamada, *J. Phys. Soc. Jpn.* **71**, 717 (2002).
- ³¹Y. Shimojo, H. Ito, T. Ishiguro, T. Kondo, and G. Saito, *J. Supercond.* **12**, 501 (1999).
- ³²H. Sato, H. Taniguchi, Y. Nakazawa, K. Kato, K. Kanoda, and A. Kawamoto, *Synth. Met.* **70**, 915 (1995).
- ³³O. Klein, S. Donovan, M. Dressel, and G. Grüner, *Int. J. Infrared Millim. Waves* **14**, 2423 (1993).
- ³⁴M. W. Coffey and J. R. Clem, *Phys. Rev. Lett.* **67**, 386 (1991).
- ³⁵S. Sridhar, B. Maheswaran, B. A. Willemsen, D. H. Wu, and R. C. Haddon, *Phys. Rev. Lett.* **68**, 2220 (1992).
- ³⁶E. C. Palm and T. P. Murphy, *Rev. Sci. Instrum.* **70**, 237 (1999).
- ³⁷D. Shoenberg, *Magnetic Oscillations in Metals* (Cambridge University Press, Cambridge, England, 1984).
- ³⁸J. Wosnitza, G. W. Crabtree, H. H. Wang, U. Geiser, J. M. Williams, and K. D. Carlson, *Phys. Rev. B* **45**, 3018 (1992).
- ³⁹L. N. Bulaevskii, *Adv. Phys.* **37**, 443 (1988).
- ⁴⁰A more detailed discussion of calculating the Pauli limit can be found at <http://physics.clarku.edu/superconductor/PauliFold/CalculatingHP.html>
- ⁴¹K. Miyagawa *et al.*, *Synth. Met.* **86**, 1987 (1997).
- ⁴²S. Wanka, J. Hagel, D. Beckmann, J. Wosnitza, J. A. Schlueter, J. M. Williams, P. G. Nixon, R. W. Winter, and G. L. Gard, *Phys. Rev. B* **57**, 3084 (1998).
- ⁴³L. N. Bulaevskii, *J. Mod. Phys. B* **4**, 1849 (1990).
- ⁴⁴Y. Shimojo, T. Ishiguro, M. A. Tanatar, A. E. Kovalev, H. Yamochi, and G. Saito, *J. Phys. Soc. Jpn.* **71**, 2240 (2002).
- ⁴⁵Jeremy Qualls of Wake Forest University made the new samples.